Diamond & Related Materials 20 (2011) 134–139

Contents lists available at ScienceDirect

Diamond & Related Materials

journal homepage: www.elsevier.com/locate/diamond

CVD diamond for spintronics ☆

M.L. Markham [a,*], J.M. Dodson [a], G.A. Scarsbrook [a], D.J. Twitchen [a], G. Balasubramanian [b], F. Jelezko [b], J. Wrachtrup [b]

[a] Element Six, Kings Ride Park, Ascot, SL5 8BP, UK
[b] 3 Physikalisches Institut, Universität Stuttgart, 70550 Stuttgart, Germany

ARTICLE INFO

Available online 27 November 2010

Keywords:
Diamond crystal
Synthetic diamond
Plasma CVD
Defect characterization
Optoelectronic properties
Detectors
Sensors

ABSTRACT

The ability to minimise, control and manipulate defects in CVD diamond has grown rapidly over the last ten years. The application which best illustrates this is probably that of quantum information processing (QIP) or 'diamond spintronics'. QIP is a rapidly growing area of research, covering diverse activities from computing and code breaking to encrypted communication. All these applications need 'quantum bits' or qubits where the quantum information can be maintained and controlled. Controlled defects in an otherwise high perfection diamond lattice are rapidly becoming a leading contender for qubits, and offer many advantages over alternative solutions. The most promising defect is the NV^- defect whose unique properties allow the state of its electron spin to be optically written to and read from. Substantial developments in the synthesis of CVD diamond have produced diamond lattices with a high degree of perfection, such that the electron spin of this centre exhibits very long room temperature decoherence times (T_2) in excess of 1 ms. This paper gives a brief review of the advantages and challenges of using CVD diamond as a qubit host. Lastly the various qubit applications being considered for diamond are discussed, highlighting the current state of development including the recent development of high sensitivity magnetometers.

1. Introduction

Defects in CVD diamond can have a profound effect on certain properties of the diamond, enabling these properties to be tailored to the specific needs of important applications. Properties sensitive to defects include optical properties such as absorption and birefringence [1,2], thermal properties such as thermal conductivity [3], and electronic properties such as carrier mobility and lifetime [4,5].

During the past few years researchers have gained control over quantum behaviour in the solid state at the level of a single spin. What was considered as a "thought experiment" a decade ago is now a reality: spins of single atoms and electrons associated with defects in diamond can be isolated, initialised, manipulated and read using optical techniques [6–8]. Diamond, due to its unique capacity to operate spin devices at room temperature offers the possibilities to create functional quantum devices for applications from nano-scale magnetic imaging to quantum computing. These abilities now enable pioneering investigations of the exploitation of fundamental quantum physics for a disruptive technology, namely diamond spintronics.

These breakthroughs have been based on the negatively charged nitrogen-vacancy (NV^-) colour centre in diamond. This paper will review the properties of diamond that underlie this work, and focus on the progress made in growing synthetic quantum purity diamond using chemical vapour deposition (CVD) with a specific emphasis on the control of point defects and isotopic composition in the diamond. These synthesis developments have lead to decoherence times of the NV^- electronic spin at room temperature of 0.6 ms in polycrystalline diamond as shown in this letter, and in excess of 1 ms in isotopically engineered single crystal samples [9]. In terms of controlling and manipulating defects, diamond spintronics is probably the most demanding of all applications. As such, it is also a key driver for improving defect control, and offers unique ways to characterise defects in diamond with very high sensitivity.

2. Why use diamond as a qubit host lattice?

In the early 1980s the potential power of quantum based computation using qubits was realised and quantum algorithms (such as Shor's factorising algorithm and Grover's search algorithm) were developed. This started the race to find quantum bits or qubits that could be controlled and engineered for quantum information processing (QIP).

Currently the range of qubits varies from non-solid state systems such as photons [10] or ion traps [11–13] to solid state systems such as quantum dots [14], superconductors [15,16] or defects in solid state materials [17–19]. An excellent review of these options and their potential for use in quantum computing is given by [20]. Obviously, if

☆ Presented at NDNC 2010, the 4th International Conference on New Diamond and Nano Carbons, Suzhou, China.

* Corresponding author. Tel.: +44 1344 638201; fax: +44 1344 638236.
E-mail address: matthew.markham@e6.com (M.L. Markham).

0925-9635/$ – see front matter © 2010 Elsevier B.V. All rights reserved.
doi:10.1016/j.diamond.2010.11.016

a suitable qubit can be generated in a stable, solid state source, this may have practical advantages over other candidates.

To be useful as a qubit, the encoded information must be retained in a quantum, rather than classical, sense for long enough for the quantum operations to be performed. For spin qubits, this retention time for their quantum state can be quantified by the transverse relaxation time, T_2. This is also known as the dephasing or, as will be used here, decoherence time.

There are two main reasons that defects in diamond form good qubits:

(i) Single defect centres can be addressed using conventional optical techniques
(ii) Defect centres can have long decoherence times at ambient temperatures.

These properties start to fulfil the DiVincenzo criteria [21]: they have the possibility to form a scalable physical system, can be written to and read from [22] and have demonstrated CNOT gates [23]. Depending on the defect being studied, the long decoherence time can be significantly longer than the gate operation time, and some defects can be initialised to form a known qubit state.

Other important results demonstrated in diamond are: a 3-qubit system, with brokering (information transfer) to longer-lived nuclear spins (in this case, a nearby ^{13}C), again at room temperature [24], and defects that can be used as single photon sources [25–27].

2.1. Diamond as a low spin lattice

Diamond offers intrinsic properties which limit the impact of spin decoherence mechanisms. These are the mechanisms through which the quantum information encoded to a specific spin is lost — interaction of that spin with its spin environment.

The main decoherence mechanism is spectral diffusion: the existence of other fluctuating spins which, through dipolar coupling to the spin qubits leads to decoherence. While the presence of electronic spins can be controlled by the purity of the material, i.e. minimising the number of intrinsic and extrinsic defect centres which have a non-zero spin, the nuclear spins are controlled by the material choice. For example, none of the three stable isotopes for GaAs is spin zero (^{69}Ga, ^{71}Ga, and ^{75}As). In diamond the major nuclear component, spin zero ^{12}C, is 98.9% naturally abundant, which gives it a significant advantage over quantum dots. The ability to grow diamonds containing only spin-free ^{12}C isotope will potentially lead to possibility of extending coherence time to ultimate limit defined by spin lattice relaxation time. However, the spin lattice relaxation time in diamond is particularly long (reaching ms for ultrapure IIa type material) [9,28].

2.2. Spin defects in diamond — the NV^- defect

Diamond colour centres have been well studied, with over five hundred characterised [29,30]. There are several diamond colour centres that have shown potential for spintronic applications including the nitrogen vacancy defect [31], the nickel–nitrogen NE8 defect [32,33] and the silicon vacancy defect [34].

The most studied diamond defect to date is the NV^- centre, shown with its associated electronic structure in Fig. 1. Its neutral state emits with a zero phonon line (ZPL) at 575 nm and has not so far been viable for spin studies. In its negative state, the nitrogen vacancy defect's electron wave function is made up of six electrons that results in an electron paramagnetic $S=1$ electron spin ground state that has a splitting of 2.88 GHz in the absence of a magnetic field. The optical transition between the spin triplet states ^3E and ^3A possesses a ZPL at 637 nm.

The electronic structure of the NV^- centre means that optical illumination generates a non-Boltzmann spin alignment of the electron spin in the ^3A ground state [35]. The precise reason for this spin polarisation is hotly debated, but is often described to be due to intersystem crossing with an intermediate singlet state: the ^3E $m_s=0$ decays radiatively with conserved spin to the ground state, while the ^3E $m_s=\pm1$ decays via the ^1A singlet state. This is non-radiative, and non-spin conserving, also ending up in the ground state $m_s=0$. Illumination with any light with a shorter wavelength than the ZPL therefore acts as an initialisation step, creating a $|0>$qubit in the ground state, with an effective micro-Kelvin electronic spin temperature even though the crystal is at room temperature.

The initialised qubit can then be manipulated by application of an appropriate length of a resonant RF pulse. Readout of the qubit typically uses confocal microscopy. NV^- defects have a large dipole moment and therefore single defects can be readily addressed [36]. The final state of the ground state qubit is inferred from the intensity of the emitted light following further excitation — $|1>$results in a low fluorescence intensity, because of the comparatively slow, non-radiative singlet decay, while $|0>$produces a high intensity, being a simple radiative transition which is rapidly re-excited, giving further emission.

These properties and successes in manipulating defects have put diamond in the frame as an important QIP material.

3. Methods

3.1. CVD diamond synthesis

Processes that require quantum control in the solid state generally place high demands on the material quality. The quality factors in a crystalline material can be intrinsic defects such as dislocations,

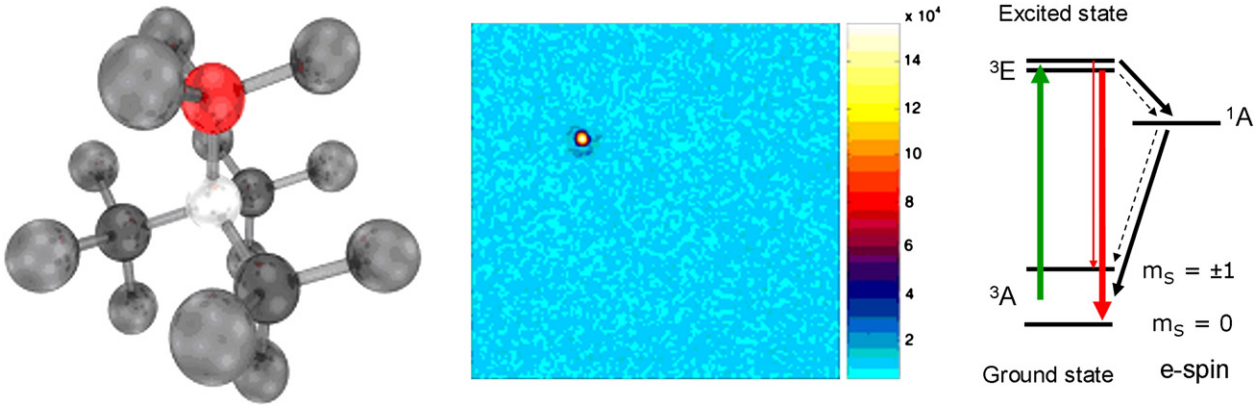

Fig. 1. Left: Nitrogen-vacancy defect in diamond and fluorescence microscopy image of high purity CVD diamond containing single nitrogen-vacancy defect. Right: Energy level scheme of the nitrogen-vacancy (NV^-) defect in diamond showing non-radiative decay from the ^3E $m_s=\pm1$ excited state.

vacancies and other abnormally bonded atoms, or extrinsic defects such as point defects involving impurities. For quantum grade diamond the main requirement is to produce material with a low level of impurities and in particular a low level of paramagnetic impurities which would otherwise act as a spin bath, interacting with the qubits.

Gas phase synthesis of diamond is particularly suited to producing high purity material, benefitting from decades of work developing high purity gases for the semiconductor industry. This complements the fundamental increase in control offered by a vacuum process in contrast to other synthesis methods (HPHT or shock wave). Within gas phase synthesis methods, two main factors influence the quality of the material — any impurities introduced by the activation method, and the degree of activation. While arc-jets provide a strongly activated (3200 K to 5000 K [37,38]) plasma for high quality diamond synthesis, the nozzles are prone to erosion, and are therefore a source of impurities in the material. Hot filament reactors provide the least activation with the peak gas temperature, which can be no higher than the filament temperature, around 2000 K [39]. This comparatively low level of gas activation, combined with the filament being a source of impurities, is consistent with there being no reports of high quality, high purity diamond being synthesised by this method. Microwave plasmas provide a high degree of activation, with peak gas temperatures of approximately 3000 K [40,41], and are excited by remote sources of power. The only sources of impurity are therefore the cold chamber walls, the gases, and any atmospheric ingress. This method has produced the highest quality of material to date.

The properties of "Electronic grade" polycrystalline diamond, grown by microwave plasma assisted CVD, have been previously reported [42,43]. Wafers of this grade are commercially available up to 120 mm diameter and 1 mm thick. The mean single substitutional nitrogen (N_s^0) concentration is below 50 ppb [44]; since polycrystalline diamond is an inhomogeneous material, with defects likely to be segregated near the grain boundaries, the in-grain nitrogen concentration is significantly lower than the mean value. Other extrinsic impurities are found to be below the SIMS detection limit (0.5 ppb for boron). The diamond lattice quality is demonstrated by a high charge collection efficiency when processed and used as a particle detector [42], and high performance when used in a surface FET [45]. These results indicate low trap densities and high charge carrier mobility.

Similar conditions can be used to synthesise both high purity polycrystalline and single crystal diamond. Typical operating pressures exceed 15 kPa, with a primarily hydrogen gas mixture; argon is present at up to 10%, and the carbon source is a few percent of CH_4. No intentional nitrogen addition is reported, and substrate temperatures are normally in the range of 750–900 °C [46]. The samples reported in this paper have been grown using microwave sources of both L-band (896–922 MHz) and S-band (2450 MHz).

An extra complication for the growth of high quality single crystal diamond comes in the need to select and prepare suitable single crystal diamond substrates, as the growth is homoepitaxial. Examples of the variation in birefringence, due to different densities of dislocation bundles, can be found in Turri et al. [1], whilst Friel et al. [2] report that reduction in dislocation bundle density is possible with careful selection and preparation of the substrate. The substrate selection aims to minimise defects which can be propagated, by the homoepitaxial growth, into the CVD layer. The substrate preparation aims to minimise defects nucleated at the substrate–CVD interface, by presenting a low damage surface on which growth is initiated. Maintaining stable, controlled growth conditions then enables good quality, high purity single crystal diamond to be synthesised. Ensemble EPR measurements indicate the bulk single substitutional nitrogen concentration of <5 ppb.

In order to synthesise samples with a reduced proportion of spin 1/2 ^{13}C, isotopically enriched ^{12}C methane is readily available. However its production method (via fractional distillation of mass 28 CO [47]) results in significantly higher nitrogen levels than can be supplied in natural abundance methane. Growth conditions that would normally produce high purity material are unsuccessful with these higher levels of source nitrogen (>3 ppm) — if the sample has too high a nitrogen concentration, extrinsic defects are re-introduced as a source of decoherence. Modification of the growth conditions is necessary to reduce the nitrogen uptake ratio in the {100}, allowing synthesis of high purity, 99.7% ^{12}C enriched single crystal diamond [48,49]. Synthesis of 99.99% ^{12}C enriched high purity single crystal diamond has also been achieved; results will be reported later.

3.2. Spin characterization

Due to the fact that the NV^- centre has a large dipole moment, individual centres can be identified and characterised using conventional confocal microscopy with optical and microwave pulses used to write to, read and manipulate the centre [50]. The simplicity of the system and the fact that diamond defects can be controlled at room temperature, mean that robust optical set-ups can be created for characterisation.

A basic confocal system consists of a 532 nm laser as the excitation source, small metal wires on the surface of the diamond connected to a signal generator as a microwave source and detectors to collect any emission [51]. Single defects can be identified using a Hanbury Brown–Twiss experiment where a single centre is identified by a characteristic anti-bunching signature in the coincidence rate [25]. Fig. 1 shows a single defect in single crystal and Fig. 2 shows single centres in polycrystalline diamond.

The spin coherence time (T_2) of a single electron spin in a NV^- centre can be probed using Hahn echo decay. Adapted to optically detected magnetic resonance, the Hahn echo pulse sequence, depicted in Fig. 3, consists of the well-known $\pi/2–\tau–\pi–\tau–\pi/2$ series of microwave pulses (τ is the variable delay between pulses) [52]. The last pulse converts the spin echo phenomenon into populations, measurable by fluorescence detection.

4. Results

4.1. Polycrystalline diamond

Here, we report for the first time long decoherence times measured in low defect density polycrystalline CVD diamond. The confocal microscopy luminescence images in Fig. 2 show a few grains in "Electronic grade" CVD diamond, which are each around 100 μm across. The grain boundaries, being comparatively defect rich, show strong luminescence. A number of the point-like defects within the grains have been confirmed to be NV^- centres, with a significant fraction being single centres (data not shown). The spatial variation within grains illustrates different defect uptake levels in different growth sectors. A clear example of a sector boundary, or the original facet edge before planarisation, runs between 1 and 2 on Fig. 2.

The higher magnification image (on the right) concentrates on one of the lower defect regions. The luminescent defect surface concentration in these sectors is of the order $10^7\,cm^{-2}$, counting over $100\,\mu m^2$ regions. The depth of field is approximately 10 μm, which corresponds to a local volume concentration of order $10^{10}\,cm^{-3}$. Despite being a polycrystalline diamond, single NV^- defects in these low defect regions have demonstrated T_2 of 600 μs when the defects are located far from grain boundaries. Defects closer to grain boundaries are effected by dipole coupling to other defects at the crystal border but this is limited to a few tens of nanometres. Hahn echo decay data for this sample, is given in Fig. 4.

4.2. Single crystal diamond

For samples with N_s^0 concentration below 1 ppb ($<1.7\times10^{14}\,cm^{-3}$) [53], the NV^- concentration is determined using confocal PL counting

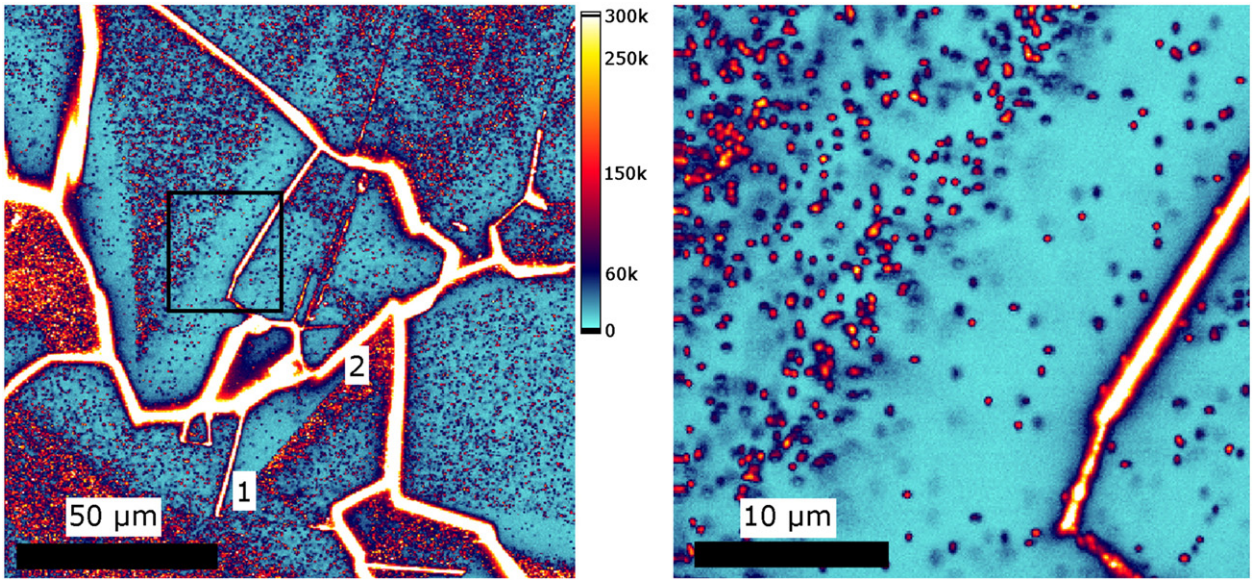

Fig. 2. Fluorescence microscopy image of "Electronic grade" polycrystalline CVD diamond containing multiple NV centres. Bright regions correspond to grain boundaries; within grains, the boundary between facets' different nitrogen uptake can be seen e.g. between points 1 and 2. Right hand figure is a higher magnification of the black square.

methods to be below 10^{10} cm^{-3}. In contrast to the polycrystalline diamond, the NV$^-$ defects are more uniformly distributed. Under these circumstances, a decoherence time of 650 μs has been measured [54]. For this natural abundance high purity diamond, most extrinsic sources of decoherence have been reduced to a very low level, primarily with low nitrogen. With the density of dislocation bundles below 10^4 cm^{-2}, and low levels of disordered bonding remaining, these intrinsic defects are no longer likely to be a dominant cause of spin decoherence.

High purity, 99.7% ^{12}C enriched single crystal diamond has been shown to possess a T_2 of 1800 μs [9]. Hahn echo decay data for this sample, and a natural abundance sample are included for comparison in Fig. 4. The dependence of T_2 on ^{12}C concentration is approximately inversely proportional to the ^{13}C concentration [54].

5. Implications and applications

The improvements in material purity and quality have led to an increase in the decoherence time as described in the previous sections. Table 1 presents these decoherence times in the context of other diamond results. In general increasing T_2 allows more time for operations and information storage and thus allows more complex processing such as that required in a quantum computer.

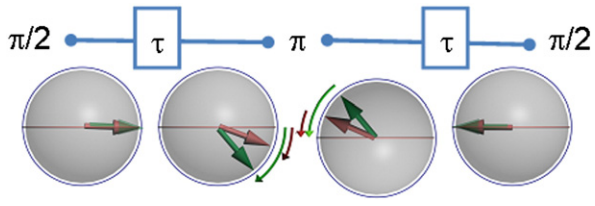

Fig. 3. Schematic illustration of spins during Hahn echo decay measurement. Starting from the left, a π/2 pulse flips the spin vectors into the equatorial plane of the Bloch sphere as shown in the first grey sphere. After a delay, τ, dephasing occurs as indicated by the separation of the green and red vectors. A rephasing π pulse is then applied prior to another π/2 pulse for readout.

The properties of the NV$^-$ defect and the advances in material quality have led to several possible applications. One of the simplest applications, that does not require high purity material, is that of a single photon source for quantum communication (or quantum key distribution). Quantum key distribution (QKD) has interest for military and commercial applications where secure information transfer is vital. Implementation of QKD has been performed with NV$^-$ centres in free space over a distance of 30 m [27]. A true single photon source is now commercially available [55]. The disadvantage of using the NV$^-$ centre as a single photon source is that it has a large emission bandwidth and non-optimal central emission wavelength however, other defects in diamond may be better candidates [33,34,56].

Another application of the NV$^-$ defect is for detection of magnetic fields as first suggested in 2005 [57]. This technique has been

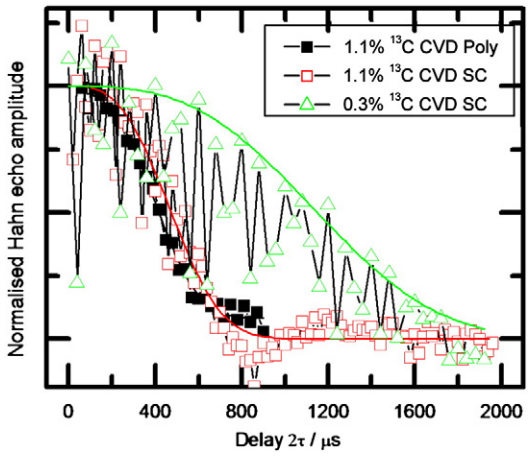

Fig. 4. Coherence time of single spins: Hahn echo fluorescence intensity decay versus time showing similar decoherence time for 1.1% ^{13}C polycrystalline (poly) and single crystal (SC) samples, and increased decoherence time for reduced ^{13}C content SC sample. The fit function represents Gaussian decay $\left(\exp\left[-\left(\frac{2\tau}{T_2}\right)^3\right]\right.$ where 2τ is the length of the echo sequence and T_2 is the coherence time [54].

Table 1
Decoherence time, T_2, of NV^- centres in different types of diamond as measured by Hahn echo decay. The effect of reducing ^{13}C content is shown by the last pair of results.

Sample details	T_2	Reference
Nanodiamond	1.5–15 μs	[50,84]
Type Ib (ensemble measurement)	3.6 μs	[85]
Selected Type IIa natural	350 μs	[52]
"Electronic grade" CVD polycrystalline	600 μs	This work
High purity CVD single crystal, 1.1% ^{13}C	650 μs	[9]
High purity CVD single crystal, 0.3% ^{13}C	1800 μs	[9]

described [58] and developed for NV^- centres in diamond [9,59–61]. There are a few different methods of implementation using either nanodiamond or diamond slabs however the basic technique is the same; the NV^- centre is optically initialised and read out; the change in the spin alignment of the NV^- centre is a function of the magnetic field. This technique has been demonstrated to have a magnetic field-integration time sensitivity as low as 4 nT $Hz^{-1/2}$ [9]. The maximum sensitivity that is obtainable depends on the decoherence time of the NV^- centre [62]. Since the technique only requires a single NV^- centre and its local environment, the measurement is possible with ~nm^3 detection volumes. This compares favourably with other techniques of comparable sensitivity such as SQUIDs and Hall probes, which can only be reduced to μm^3 volumes. To get a feeling of the sensitivity, an isolated electron produces a field of 3 μT at about 10 nm, while a proton would produce 3 nT at a distance of 10 nm.

The last application considered using NV^- centres is a fully scalable quantum computer. For this to be achieved significant advances in the processing of diamond are required, along with controlling the location and properties of NV^- defects. While the scalable quantum computer is still a long way off the fact that NV^- centres have demonstrated long decoherence times at room temperature, can be optically written to and read from, and can be coupled [19] are three of the basic criteria necessary to make a quantum computer [21,63]. En route to the quantum computer may be a quantum repeater, which would be necessary for long distance QKD. Amongst other things, this requires two qubit entanglement; this has now been achieved by coupling to local nuclear spins [64,65].

6. Challenges for the future

There remain many challenges on the way to fully implementing diamond in these applications, many of which are related to its extreme properties.

Using colour centres and needing to couple the photons outside of the diamond means that diamond's high refractive index is an issue. If simple slabs of diamond are used, the light collection efficiency is poor (below 5%). However a number of approaches are improving the light collection by shaping the diamond, including fabrication of solid immersion lenses [44], focused ion beam milling, controlled damage implantation and ICP etching [28,66,67]. Without shaping the diamond, the light can be coupled directly into GaP [68] or plasmonic waveguides [69–71].

While NV^- centres have an ideal electronic structure for spintronic applications, the photons emitted are not ideal: 637 nm suffers comparatively high losses in optical fibres and is not suitable for daylight free space transmission. Also, 96% of photons from the NV^- defect are emitted into the phonon sideband, therefore only 4% are suitable for some QIP schemes. This fraction can be improved by constructing a cavity around the defect which limits the number of permissible optical modes [72–75].

In addition to the NV^- defect, many other defects have demonstrated useful properties, such as NE8 (a Ni atom and 4 adjacent nitrogen atoms [32]) and another as yet unidentified Cr defect [76]. Ni–Nitrogen defects have been used to demonstrate daylight free space transmission [77]. NE8 and the Cr defect both emit in the near infra-red from 744 nm to 800 nm [33,56] with the potential for improved fibre transmission. They both have narrow ZPL linewidths and nanosecond lifetimes. In contrast to NV^-, more than 70% of their emission is into the ZPL [31,33,78]; however none of these has yet shown the desirable spin polarisation properties of NV^-.

Finally, the best performing defects are those which are "found" in as grown high purity CVD material. Even these still show some sensitivity to variations in local environment [79] and are therefore distinguishable unless they can be Stark shift tuned (e.g. work by Tamarat et al. [80]), or the underlying crystal uniformity can be improved. However applications would ideally like to know the defect locations *a priori*. Implantation with ~15 nm resolution has been demonstrated [9,19,81–83]. Using implanted centres in high purity diamond offers the possibility to construct a quantum register [19]. However the yield of formation of NV^- centres (21%) and their limited decoherence times need to be improved over the current state-of-the-art. One potential route is for two-stage, two temperature anneals — around 800 °C to form the defect centres by vacancy diffusion, followed by a higher temperature to heal some of the lattice damage. But just as diamond's stiff lattice presents the challenges in annealing out implantation damage, it also helps by providing the ultimate stability of defects once they have formed.

7. Summary

The level of work performed using diamond for QIP is gathering pace with diamond based QIP products already commercially available (e.g. the single photon source). Commercially produced high purity diamond suitable for this area of research is routinely manufactured. The development of near isotopically pure low defect CVD diamond (99.7% and 99.99% ^{12}C) demonstrates that control of relevant spin defects is possible, although more improvements in the material may still be required.

Defects in diamond meet many of the DiVincenzo criteria. The NV^- defect has an initialisation state, confocal microscopy allows individual qubit measurements, defects emit single photons and decoherence times are significantly longer than gate operation times. However many issues will need to be addressed to produce a scalable diamond based quantum computer. Challenges will include growth and engineering diamond that emits indistinguishable photons, and constructing microcavity devices with which to exercise control over the spontaneous emission process. However the possibility of near term applications such as magnetic field sensing and QKD also make diamond based QIP of interest as a commercial product on the way to scalable quantum computing.

With all these possibilities and ambient temperature operation, diamond is fast becoming an exciting spintronic material for fundamental science and novel applications.

Acknowledgement

This work is supported by the European Commission through the EQUIND (contract IST-034368) project.

References

[1] G. Turri, et al., Opt. Eng. 46 (2007) 064002.
[2] I. Friel, S.L. Clewes, H.K. Dhillon, N. Perkins, D.J. Twitchen, G.A. Scarsbrook, Diamond Relat. Mater. 18 (2009) 808.
[3] T.R. Anthony, W.F. Banholzer, J.F. Fleischer, Wei Lanhua, P.K. Kuo, R.L. Thomas, R.W. Pryor, Phys. Rev. B 42 (1990) 1104.
[4] A. Lohstroh, P.J. Sellin, S.G. Wang, A.W. Davies, J. Parkin, R.W. Martin, P.R. Edwards, Appl. Phys. Lett. 90 (2007) 102111.
[5] C.E. Nebel, M. Stutzmann, in: M.H. Nazare, A.J. Neves (Eds.), Properties, Growth and Applications of Diamond, INSPEC, The IEE, London, 2001, p. 40.
[6] F. Jelezko, J. Wrachtrup, in: S. Koizumi, C. Nebel, M. Nesladek (Eds.), Physics and Applications of CVD Diamond, Wiley, Germany, 2008, p. 257.
[7] M.V.G. Dutt, M.D. Lukin, et al., Science 316 (2007) 5829.
[8] A. Batalov, J. Waratchrup, Phys. Rev. Lett. 100 (2008) 077401.

[9] G. Balasubramanian, et al., Nat. Mater. 8 (2009) 383.
[10] J.L. O'Brien, G.J. Pryde, A.G. White, T.C. Ralph, D. Branning, Nature 426 (2003) 264.
[11] D. Leibfried, B. DeMarco, V. Meyer, D. Lucas, M. Barrett, J. Britton, W.M. Itano, B. Jelenkovi, C. Langer, T. Rosenband, D.J. Wineland, Nature 422 (2003) 412.
[12] F. Schmidt-Kaler, H. Häffner, M. Riebe, S. Gulde, G.P.T. Lancaster, T. Deuschle, C. Becher, C.F. Roos, J. Eschner, R. Blatt, Nature 422 (2003) 408.
[13] R. Blatt, D. Wineland, Nature 453 (2008) 1008.
[14] X. Li, Y. Wu, D. Steel, D. Gammon, T.H. Stievater, D.S. Katzer, D. Park, C. Piermarocchi, L.J. Sham, Science 301 (2003) 809.
[15] T. Yamamoto, Y.A. Pashkin, O. Astafiev, Y. Nakamura, J.S. Tsai, Nature 425 (2003) 941.
[16] J. Clarke, F.K. Wilhelm, Nature 453 (2008) 1031.
[17] A.M. Stoneham, A.J. Fisher, P.T. Greenland, J. Phys. Condens. Matter 15 (2003) L447.
[18] F. Jelezko, I. Popa, A. Gruber, J. Wrachtrup, Appl. Phys. Lett. 81 (2002) 2160.
[19] P. Neumann, et al., Nat. Phys. 6 (2010) 249.
[20] T.D. Ladd, F. Jelezko, R. Laflamme, Y. Nakamura, C. Monroe, J.L. O'Brien, Nature 464 (2010) 45.
[21] D.P. DiVincenzo, Fortschr. Phys. 48 (2000) 771.
[22] R. Hanson, F.M. Mendoza, R.J. Epstein, D.D. Awschalom, Phys. Rev. Lett. 97 (2006) 087601.
[23] F. Jelezko, T. Gaebel, I. Popa, M. Domhan, A. Gruber, J. Wrachtrup, Phys. Rev. Lett. 93 (2004) 130501.
[24] P. Neumann, N. Mizuochi, F. Rempp, P. Hemmer, H. Watanabe, S. Yamasaki, V. Jacques, T. Gaebel, F. Jelezko, J. Wrachtrup, Science 320 (2008) 1326.
[25] R. Brouri, A. Beveratos, J.-P. Poizat, P. Grangier, Opt. Lett. 25 (2000) 1294.
[26] C. Kurtsiefer, S. Mayer, P. Zarda, H. Weinfurter, Phys. Rev. Lett. 85 (2000) 290.
[27] R. Alleaume, F. Treussart, G. Messin, Y. Dumeige, J.-F. Roch, A. Beveratos, R. Brouri-Tualle, J.-P. Poizat, P. Grangier, New J. Phys. 6 (2004) 92.
[28] M.V. Gurudev Dutt, L. Childress, L. Jiang, E. Togan, J. Maze, F. Jelezjo, A.S. Zibrov, P.R. Hemmer, M.D. Lukin, Science 316 (2007) 1312.
[29] A.M. Zaitsev, Phys. Rev. B 61 (2000) 12909.
[30] A.M. Zaitsev, Optical Properties of Diamond. A Data Handbook, Springer-Verlag, Germany, 2001.
[31] J. Wrachtrup, F. Jelezko, J. Phys. Condens. Matter 18 (2006) S807.
[32] V.A. Nadolinny, A.P. Yelisseyev, J.M. Baker, M.E. Newton, D.J. Twitchen, S.C. Lawson, O.P. Yuryeva, B.N. Feigelson, J. Phys. Condens. Mat. 11 (1999) 7357.
[33] T. Gaebel, I. Popa, A. Gruber, M. Domhan, F. Jelezko, J. Wrachtrup, New J. Phys. 6 (2004) 98.
[34] C. Wang, C. Kurtsiefer, H. Weinfurter, B. Burchard, J. Phys. B: At. Mol. Opt. Phys. 39 (2006) 37.
[35] J. Harrison, M.J. Sellars, N.B. Manson, J. Lumin. 107 (2004) 245.
[36] A. Gruber, A. Drabenstedt, C. Tietz, L. Fleury, J. Wrachtrup, C. von Borczyskowski, Science 276 (1997) 2012.
[37] J. Luque, W. Juchmann, E.A. Brinkman, J.B. Jeffries, J. Vac. Sci. Technol. A 16 (1998) 397, doi:10.1116/1.581037.
[38] C.J. Rennick, J. Ma, J.J. Henney, J.B. Wills, M.N.R. Ashfold, A.J. Orr-Ewing, Yu.A. Mankelevich, J. Appl. Phys. 102 (2007) 063309.
[39] J.A. Smith, E. Cameron, M.N.R. Ashfold, Y.A. Mankelevich, N.V. Suetin, Diamond Relat. Mater. 10 (2001) 358.
[40] J. Ma, J.C. Richley, M.N.R. Ashfold, Yu.A. Mankelevich, J. Appl. Phys. 104 (2008) 103305.
[41] K. Hassouni, A. Gicquel, Modeling of Moderate Pressure Microwave Plasmas Used for Diamond Deposition: Collisional Data Required for Process Simulation AIP Conf. Proc. 636, 61, 2002, doi:10.1063/1.1516324.
[42] W. Adam, et al., Nucl. Instrum. Meth. Phys. Res. A 514 (2003) 79.
[43] R.S. Wallny, Nucl. Instrum. Meth. Phys. Res. A 582 (2007) 824.
[44] R.S. Balmer, et al., J. Phys. Condens. Matter 21 (2009) 364221.
[45] K. Ueda, M. Kasu, Y. Yamauchi, T. Makimoto, M. Schwitters, D.J. Twitchen, G.A. Scarsbrook, S.E. Coe, IEEE Electron Device Lett. 27 (2006) 570.
[46] J. Isberg, J. Hammersberg, E. Johansson, T. Wikstrom, D.J. Twitchen, A.J. Whitehead, S.E. Coe, G.A. Scarsbrook, Science 297 (2002) 1670.
[47] J. Faught, Private communication (2006) (Spectra Gases, USA).
[48] Scarsbrook, Twitchen and Markham WO/2010/010344.
[49] Scarsbrook, Twitchen and Markham WO/2010/010352.
[50] F. Jelezko, T. Gaebel, I. Popa, A. Gruber, J. Wrachtrup, Phys. Rev. Lett. 92 (2004) 076401.
[51] A. Dräbenstedt, L. Fleury, C. Tietz, F. Jelezko, S. Kilin, A. Nizovtzev, J. Wrachtrup, Phys. Rev. B 60 (1999) 11503.
[52] T. Gaebel, et al., Nat. Phys. 2 (2006) 408.
[53] D.J. Twitchen, A.J. Whitehead, S.E. Coe, J. Isberg, J. Hammersberg, T. Wilkstrom, E. Johansson, IEEE Trans. Electron Devices 51 (2004).
[54] N. Mizuochi, P. Neumann, F. Rempp, J. Beck, V. Jacques, P. Siyushev, K. Nakamura, D.J. Twitchen, H. Watanabe, S. Yamasaki, F. Jelezko, J. Wrachtrup, Matter Mater. Phys. 80 (2009) 041201.
[55] www.qcvictoria.com,15/4/10.
[56] I. Aharonovich, S. Castelletto, D.A. Simpson, A.D. Greentree, S. Prawer, Phys. Rev. A 81 (2010) 043813.
[57] B.M. Chernobrod, G.P. Berman, J. Appl. Phys. 97 (2005) 014903.
[58] C.L. Degan, Appl. Phys. Lett. 92 (2008) 243111.
[59] J.M. Taylor, P. Cappellaro, L. Childress, L. Jiang, D. Budker, P.R. Hemmer, A. Yacoby, R. Walsworth, M.D. Lukin, Nat. Phys. 4 (2008) 810.
[60] J.R. Maze, et al., Nature 455 (2008) 644.
[61] G. Balasubramanian, et al., Nature 455 (2008) 648.
[62] D.J. Wineland, J.J. Bollinger, W.M. Itano, F.L. Moore, D.J. Heinzen, Phys. Rev. A 46 (1992) R6797.
[63] A. Marshall Stoneham, et al., J. Phys. Condens. Matter 21 (2009) 364222.
[64] A.A. Bukach, Kilin S. Ya, Opt. Spectrosc. 103 (2007) 202.
[65] P. Olivero, et al., Adv. Mater. 17 (2005) 2427.
[66] M.P. Hiscocks, K. Ganesan, B.C. Gibson, S.T. Huntington, F. Ladouceur, S. Prawer, Opt. Express 16 (2008) 19512.
[67] C. Lee, E. Gu, M. Dawson, I. Friel, G. Scarsbrook, Diamond Relat. Mater. 17 (2008) 1292.
[68] K.-M.C. Fu, C. Santori, P.E. Barclay, I. Aharonovich, S. Prawer, N. Meyer, Appl. Phys. Lett. 93 (2008) 234107.
[69] D.E. Chang, A.S. Sørensen, P.R. Hemmer, M.D. Lukin, Phys. Rev. Lett. 97 (2006) 053002.
[70] D.E. Chang, A.S. Sørensen, P.R. Hemmer, M.D. Lukin, Phys. Rev. B 76 (2007) 035420.
[71] Kolesov, et al., Nat. Phys. 5 (2009) 470.
[72] C.-H. Su, A.D. Greentree, L.C.L. Hollenberg, Opt. Express 16 (2008) 6240.
[73] S. Tomljenovic-Hanic, M.J. Steel, C. Martijn de Sterke, J. Salzman, Opt. Express 14 (2006) 3556.
[74] C.F. Wang, R. Hanson, D.D. Awschalom, E.L. Hu, T. Feygelson, J. Yang, J.E. Butler, Appl. Phys. Lett. 91 (2007) 201112.
[75] C.F. Wang, Y.-S. Choi, J.C. Lee, E.L. Hu, J. Yang, J.E. Butler, Appl. Phys. Lett. 90 (2007) 081110.
[76] I. Aharonovich, S. Castelletto, B.C. Johnson, J.C. McCallum, D.A. Simpson, A.D. Greentree, S. Prawer, Phys. Rev. B 81 (2010) 121201.
[77] E. Wu, V. Jacquesa, F. Treussarta, H. Zengb, P. Grangierc, J.-F. Roch, J. Lumin. 119–120 (2006) 19.
[78] I. Aharonovich, C. Zhou, A. Stacey, J. Orwa, S. Castelletto, D. Simpson, A.D. Greentree, F. Treussart, J.-F. Roch, S. Prawer, Phys. Rev. B 79 (2009) 235316.
[79] C. Santori, Private communication (2010) (HP labs, USA).
[80] Ph. Tamarat, et al., Phys. Rev. Lett. 97 (2006) 083002.
[81] D.M. Toyli, C.D. Weis, G.D. Fuchs, T. Schenkel, D.D. Awschalom, Nano Lett. 10 (2010) 3168.
[82] F.C. Waldermann, et al., Diamond Relat. Mater. 16 (2007) 1887.
[83] C. Santori, P.E. Barclay, K.-M.C. Fu, R.G. Beausoleil, Phys. Rev. B 79 (2009) 125313.
[84] J.R. Rabeau, A. Stacey, A. Rabeau, S. Prawer, F. Jelezko, I. Mirza, J. Wrachtrup, Nano Lett. 7 (2007) 3433.
[85] F.T. Charnock, T.A. Kennedy, Phys. Rev. B 64 (2001) 041201.